GoldenGate Journal of Science & Technology 2017, 3: 7 - 14 ©GJST
ISSN 2505-0656 (Print)

Physics

STUDY ON PHASE TRANSITION BEHAVIOR OF ELECTRIC PROPERTIES OF $Pb_{1-x}La_xZrTiO_3$ (x = 0, 0.5) CERAMICS.

Ganesh Raj Bajgain[1] and Bhadra Pokharel[1,2]*
[1]Department of Physics, GoldenGate International College, Battisputali, Kathmandu, Nepal
[2]Department of Engineering Physics, Institute of Engineering, Pulchowk, Lalitpur, Nepal
[*]Correspondence: grbajgain@yahoo.com

Abstract

$Pb_{1-x}La_xZrTiO_3$ (x = 0, 0.5) (PLZT) powders are synthesized using a dry route involving solid state thermo-chemical reaction in a mixture of $PbCO_3$, La_2O_3, ZrO_2 and TiO_2. The powders are calcined at temperature 750℃ for six hours and are compacted to pellets using hydraulic press. The samples are then sintered at temperature 1150℃ for 3 hours to achieve above 96% of theoretical density. The structure of samples as obtained by XRD is cubic even scanned for tetragonal for both PLZT50 and PLZT100 as confirmed by lattice parameter determination using UNIT CELL software. It is observed that PLZT samples revel dielectric anomaly around 77℃ and 48℃ for PLZT50 and PLZT100 respectively, which are the transition temperature from ferroelectric to paraelectric phase during heating mode at frequency 100 KHz. The peak values of dielectric data in cooling mode are higher than heating mode, which gives the negligible thermal hysteresis of 2℃ and 1℃ for PLZT50 and PLZT100 samples. The Curie temperature obtained from Curie-Weiss behavior for PLZT samples are similar to the transition temperature, revealing second order type phase transition or relaxor. The value of obtained from Curie-Weiss like behavior of PLZT samples are more than one, which indicate that the ferroelectric phase transition is deviating towards diffuse or relaxor type phase transition. The activation energy and resistivity of PLZT samples are obtained from the analysis of resistance data increase with the increase in composition. The impedance spectroscopy data confirm the result of phase transitions obtained from dielectric data.

***Keywords**: Perovskite; Dielectric properties; Ferroelectric properties; Thermal hysteresis; Phase Transition; Impedance spectroscopy.*

Introduction

Piezoelectric materials especially lead based materials; have been widely studied for their direct and indirect piezoelectric effects, useful in different applications (sensors, actuators transducers, and nano-positioners) because of their reliable, repeatable and reasonably good electrical properties (Jaffe B. et al 1972, Priya et al 2007). PLZT is a transparent ferroelectric ceramics formed by doping La^{+3} ions on the A site of lead zicronate titanate (PZT). The PLZT ceramics have perovskite structure with chemical formula ABO_3. The transparent nature of PLZT has led to its use in electro-optic application (Haertling et al 1999). The two factors are responsible for getting a transparent PLZT ceramics are, the reduction in the anisotrophy of the PZT crystal structure by the substitution of La^{+3} and the ability to get a pore free ceramics by either hot pressing or liquid phase sintering.

The general formula for PLZT is given by $(Pb_{1-x}La_x)(Zr_{1-y}Ti_y)_{1-\frac{x}{4}}O_3V^B_{0.25x}O_3$ and $(Pb_{1-x}La_x)_{0.5x}(Zr_{1-y}Ti_y)V^A_{0.5x}O_3$. The first formula assumes that La^{+3} ions go to the A site and vacancies (V^B) are created on the B site to maintain charge balance. The second formula assumes that vacancies are created on the A site. The actual structure may be a combination of A and B site vacancies. The electro optic application of PLZT ceramics depends on their composition. PLZT ceramics compositions in the tetragonal phase (F_T) region have a hysteresis loop with a very high coercive field (E_C). Materials with this composition exhibits linear electro-optic behavior for $E < E_C$. PLZT ceramics composition in the rhombohedral ferroelectric phase (FR) region on the PLZT phase diagram have loops with low coercive field. These ceramics are useful for optical memory applications (Cross et al 1987, Dai et al 1992).

PLZT ceramics compositions with the relaxor ferroelectric behavior are characterized by a slim hysteresis loop figure. PLZT show large quadratic electro-optic effects which are used for making flash protecting goggles to shield from intense radiation. This is one of the biggest application of the electro-optic effect shown by the transparent PLZT ceramics. The PLZT ceramics in the antiferroelectric region show a hysteresis loop expected from an antiferroelectic material. This component are used for memory

applications (Ahmad et al 2011, Xu et al 1991). The complex impedance spectroscopy (CIS) is very convenient and powerful experimental tool to correlate the electrical and structural characteristics in polycrystalline oxides. In this paper we present the study of phase transition behavior of PLZT ceramic samples by electric study.

Materials and Methods

This work synthesized of $Pb_{1-x}La_xZrTiO_3$ (x = 0, 0.5) powders by dry-route method involving solid state thermo-mechanical reaction between $PbCO_3$ (98%), La_2O_3 (99.9%), ZrO_2 (98.8%), and TiO_2 (98%) powders. These compositions in powder form were mixed in desired molar ratios properly in acetone. These solid mixtures was milled for 6 hours in indigenously designed ball-mill to produce a final powder. The mixture was dried and then calcined at 750°C for 6 hours in an alumina crucible. The calcined samples so obtained was again crushed into fine powder adding acetone for 1 hour after that added with 2% PVA (Poly-vinyl alcohol) then compacted in the form of pellets in a steel die. The green pellets were heated at 500°C for 3 hours to burn of the binding agent. After burning of binding agent, pellets (green pellets) of both pure and lanthanum doped were sintered for 3 hours at optimum temperature of 1150°C. Silver paste was painted as an electroding material at 500°C for 30 minutes to measure the dielectric properties determined by a HIOKI 3532-50 LCR HI-TESTER. The structure was studied by using D2 Phaser XRD from NAST.

Results and Discussion

A) Crystal Structure

The crystalline structural parameters were determined using X-ray diffraction data. The strong perovskite reflections can be induced with respect to a tetragonal structure (Zhigang et al 1990, Isupov et al 1975) as shown in figure (1 and 2). The lattice parameters for $Pb_{1-x}La_xZrTiO_3$ (x = 0, 0.5) were calculated for tetragonal phase by embedded into the computer program Unit cell (1997). The pattern shows the formation of single phase structure for both PLZT50 (c/a = 1.024) and PLZT100 (c/a = 1.016) however, being equal to one. The tetragonality of the samples indicates the cubic phase of the samples which matches with the report of result (Keve et al 2011). The single and sharp X-ray diffraction peaks, which are quite different in position and intensity from those of ingredients, confirm the formation of single phase new compound but presence of the extra unindexed sharp peaks may be due to impurities present in our samples during synthesis.

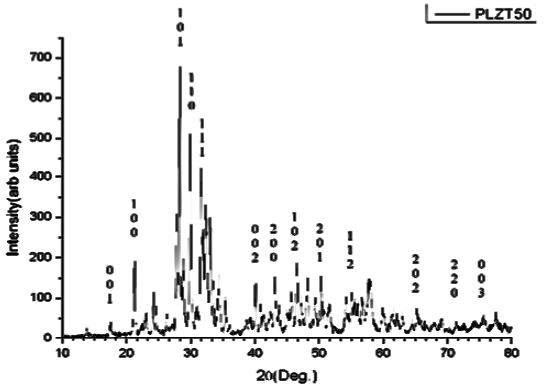

Figure 1: XRD patterns of PLZT50 sample.

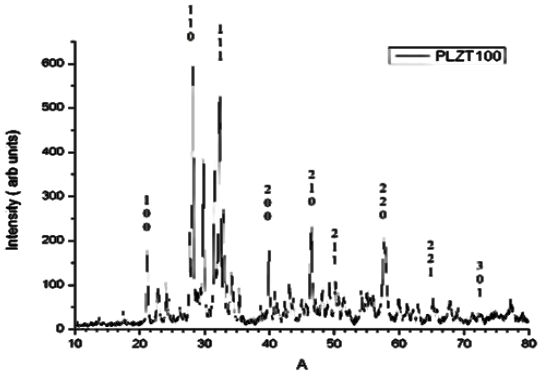

Figure 2: XRD patterns of PLZT100 sample.

B) Dielectric Measurement

1. Ferroelectric to paraelectric phase transition

The dielectric measurement were carried out at different temperatures and different frequencies. For the samples PLZT50 and PLZT100, the ferroelectric to paraelectric phase transition during heating mode occurs at temperatures 77°C and 48°C respectively. The variation of ε_r' with temperature during heating mode for samples PLZT50 and PLZT100 at 100 KHz are shown in figure (3 and 4).

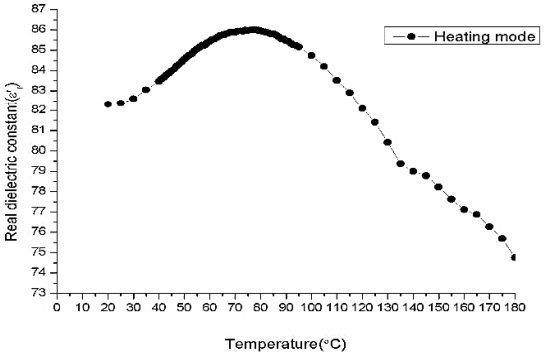

Figure 3: Variation of real part of dielectric constant with temperature at 100 KHz for PLZT50 during heating mode.

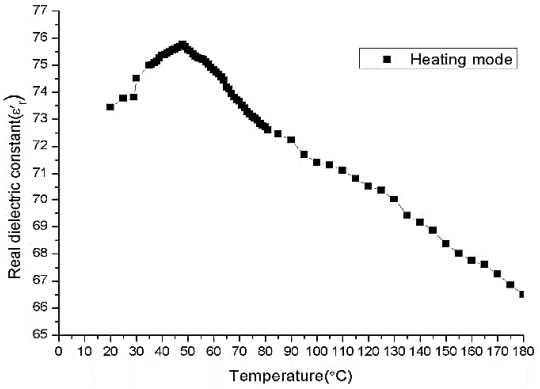

Figure 4: Variation of real part of dielectric constant with temperature at 100 KHz for PLZT100 during heating mode.

The peak value of dielectric constant for heating mode are 85.98 and 75.75 for PLZT50 and PLZT100 samples whereas at 30℃ are 82.60 and 74.52 for respective samples. The reported data (Felix et al 2013) of PLZT are similar to this result, the transition temperature and Curie temperature are 70℃ and 15℃ for PLZT. It is observed that the substitution of La^{+3} concentration in PLZT lowers the ferroelectric to paraelectric phase transition temperature and is almost linear. The imaginary part also shows the same behavior. The transition temperature of real part of dielectric constant is not exactly same as that of imaginary part of sample PLZT50, which indicates that the ferroelectric transition is relaxor type but for PLZT100, the transition temperature of ε_r' and ε_r'' are nearly same representing the regular type phase transition, which can also be confirmed by the sharpness of the peak.

2. Thermal hysteresis

The hysteresis is obtained from the difference between the transition temperatures during heating and cooling mode i.e. gives the values of thermal hysteresis. Figure (5 and 6) illustrates the variation of real part and imaginary part of dielectric constants for both heating and cooling modes at frequency 100 KHz for samples PLZT50 and PLZT100 respectively.

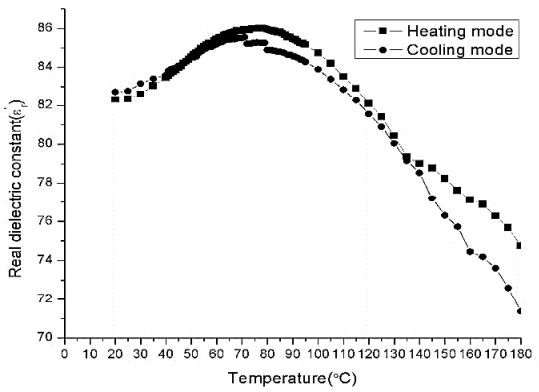

Figure 5: Variation of real part of dielectric constant with temperature at 100 KHz for PLZT50 during heating and cooling mode.

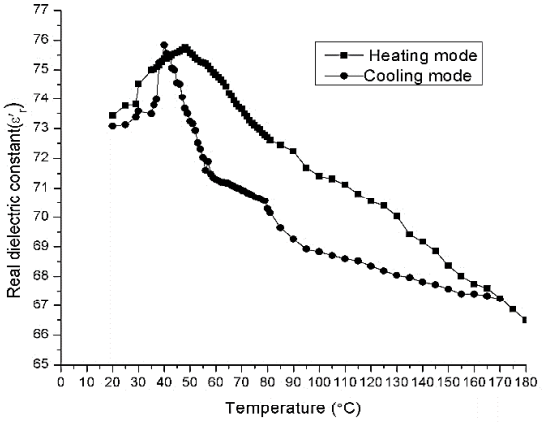

Figure 6: Variation of real part of dielectric constant with temperature at 100 KHz for PLZT100 during heating and cooling mode.

The value of thermal hysteresis observed in PLZT50 is 2℃ but for PLZT100 is 1℃, which are within the accuracy of our thermometer so there is no hysteresis.

However, the non-existence of thermal hysteresis indicates the ferroelectric transition may be second order type or relaxor in PLZT samples. The figures (5 and 6) clearly shows that the thermal hysteresis curves are not effective which is also expected in relaxor phase transition.

3. Frequency dependence of dielectric data

We have also carried out the dielectric measurement of the samples with respect to frequencies at various temperatures as shown in figure (7 and 8). The variation of peak values of dielectric constant at transition temperature and at temperature 30℃ with different frequencies are listed in the table 1 and 2.

Table 1: Values of real part of dielectric constant at 30℃ and peak temperature at different frequencies for PLZT50 sample.

frequency	ε_r' at temp. 30℃	ε_r' at peak temp.	Tc
100 KHz	82.60	86.00	77˚C
500 KHz	77.21	80.89	79˚C
600 KHz	76.11	78.95	82˚C
700 KHz	74.96	77.88	83˚C
800 KHz	72.78	76.32	80˚C
900 KHz	74.13	77.52	78˚C
1000 KHz	74.59	78.01	76˚C

Table 2: Values of real part of dielectric constant at 30℃ and peak temperature at different frequencies for PLZT100 sample.

frequency	ε_r' at temp.30℃	ε_r' at peak temp.	Tc
10 KHz	87.51	88.93	48˚C
100 KHz	74.52	75.75	48˚C
500 KHz	66.74	79.00	53˚C
1000 KHz	64.05	71.29	51˚C
2000 KHz	58.87	69.54	50˚C
3000 KHz	56.91	67.94	51˚C
4000 KHz	56.76	64.82	49˚C

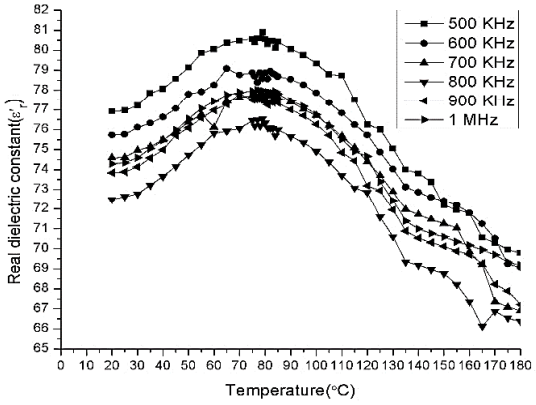

Figure 7: Variation of real part of dielectric constant with temperature at different frequencies for PLZT50.

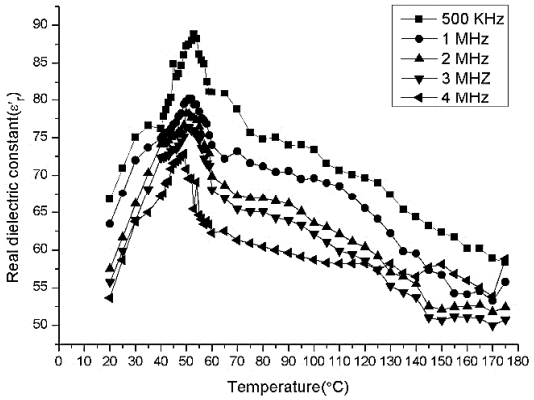

Figure 8: Variation of real part of dielectric constant with temperature at different frequencies for PLZT100.

The figures and tables show that the transition temperatures are different with the frequency which confirms that the phase transition of the samples is relaxor type. It is also noted that the differences of transition temperatures for PLZT50 is 6°C and PLZT100 is only 5°C, which confirms that PLZT50 is perfect relaxor but PLZT100 is tending towards relaxor only due being undoped PZT.

Figure (9 and 10) shows the variation of real part of dielectric constant as a function of natural log of frequency at different temperatures for PLZT50 and PLZT100 respectively. It is evident from these figures that the real part of dielectric (ε_r') data decreases with the increase of frequency. It is also noted that the dielectric data decreases with temperature up to transition temperature then starts to increase. In the frequency dependence measurements, the dielectric data decreases up to frequency 900 KHz and then it starts increasing due to anomalous dispersion effect in the samples.

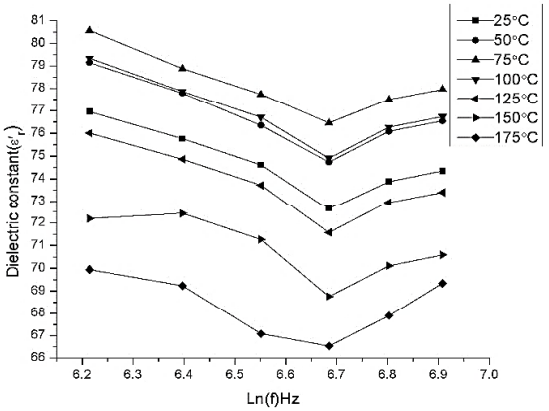

Figure 10: Variation of real part of dielectric constant as a function of frequency (ln) for different temperatures for PLZT50 sample.

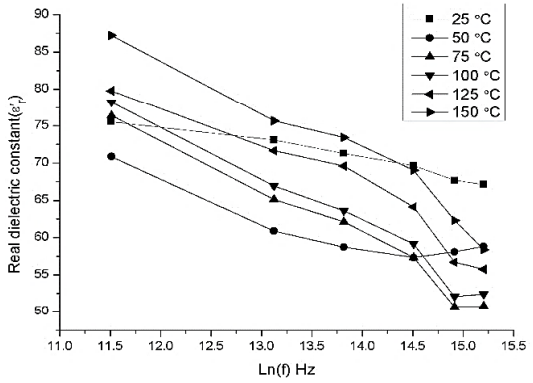

Figure 10: Variation of real part of dielectric constant as a function of frequency (ln) for different temperatures for PLZT100 sample.

The real part of dielectric constant represents the static part of the dipoles of dielectric whereas the dynamic part of dipoles is represented by imaginary part of dielectric constant which provides good knowledge of kinetic properties of dipoles (Chelkowski et al 1983, Perantie et al 2014).

4. Curie-Weiss Law

The dielectric constant of samples exhibits Curie-Weiss behavior with temperature at very close to transition temperature (Yasuda et al1996, Shvartsman et al 2006) followed by the relation:

$$\varepsilon_r' = \frac{C}{T - T_0}$$

Where C is the Curie constant and T_0 is Curie temperature. The validity of Curie-Weiss law for PLZT samples are demonstrated in figures (11 and 12), which shows the variation of dielectric stiffness $(1/\varepsilon_r')$ with temperature.

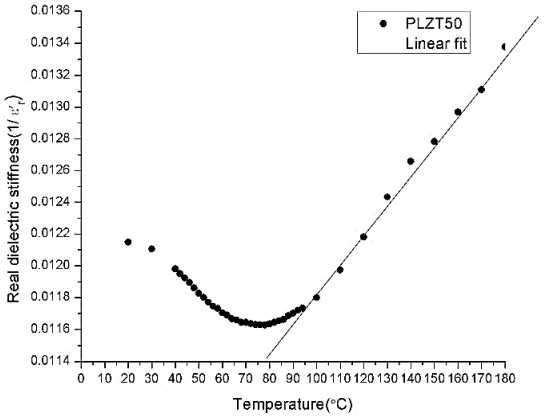

Figure11: The variation of dielectric stiffness $(1/\varepsilon_r')$ with temperature for PLZT50 at 100 KHz.

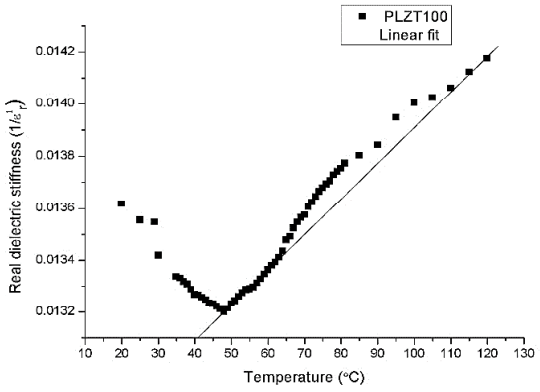

Figure 12: The variation of dielectric stiffness $(1/\varepsilon_r')$ with temperature for PLZT100 at 100 KHz.

From these figures (11 and 12), we calculated the Curie constant using the slope of the fitted straight line. The observed value of Curie constant for PLZT50 and PLZT100 are; 602.00 ^{0}C and 680.16 ^{0}C. The Curie temperatures observed from the above plots for PLZT50 and PLZT100 are 77 ^{0}C and 41 ^{0}C respectively, are the intercept values of X-axis in the $1/\varepsilon_r'$ versus temperature plots.

The Curie temperature of our sample is nearly same as that of transition temperature in the ferroelectric to the paraelectric phase which is the characteristics of the second order transition (Liu et al 1972). From these figures, it is also evident that the deviation from Curie-Weiss law is marked in PLZT50 and PLZT100 confirming the phase transition tending towards diffuse type phase transition or relaxor from regular type relaxor.

5. Modified Curie-Weiss law

To confirm the diffuseness of the phase transition, modified Curie-Weiss law proposed by Uchino and Nomura (Uchino et al 1982) is used. This is defined as,

$$\frac{1}{\varepsilon_r'} = \frac{1}{\varepsilon_m'} + \frac{(T - T_C)^\gamma}{C}$$

Where γ and C are assumed to be constant. The parameter γ gives the information on the character of phase transition. The plot of $\ln\left(\frac{1}{\varepsilon_r'} - \frac{1}{\varepsilon_m'}\right)$ vs $\ln(T - T_c)$ is shown in figure (13 and 14).

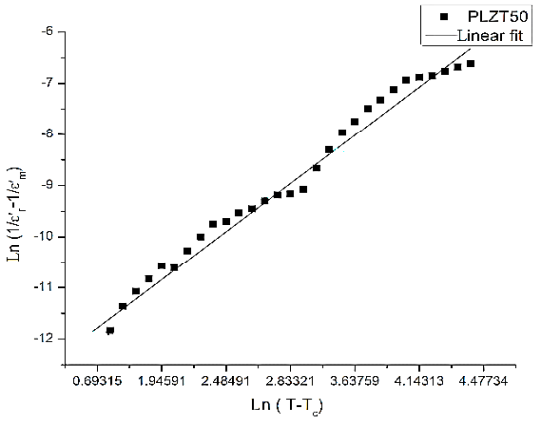

Figure 13: Variation of $\ln(\frac{1}{\varepsilon_r'} - \frac{1}{\varepsilon_m'})$ with $\ln(T\text{-}T_C)$ for PLZT50 at 100 KHz.

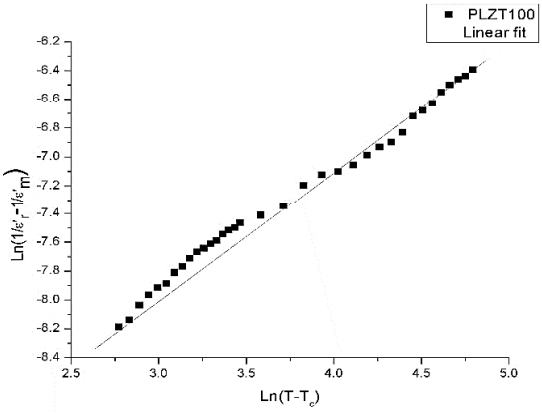

Figure 14: Variation of $\ln(\frac{1}{\varepsilon_r'} - \frac{1}{\varepsilon_m'})$ with $\ln(T\text{-}T_C)$ for PLZT100 at 100 KHz.

It is evident from the graph, the values of slope i.e., γ are 1.645 and 1.598 for sample PLZT50 and PLZT100 respectively. This confirms that the phase transition in PLZT50 is diffused or relaxor type, whereas sample PLZT100 is also tending towards relaxor type (Zhi et al 2002) because the value of γ for PLZT100 is less than PLZT50.

C) Impedance Spectroscopy

1. Resistance measurement

We have also carried out the resistance as a function of temperature with the help of the HIOKI 3532-50 LCR HITESTER. Figure (16 and 17) shows the variation of resistances with temperature during heating mode at frequency 100 KHz. By using the variation of resistivity with temperature, we use Arrhenius-type distribution in resistivity i.e.

$$\rho = \rho_0 \exp\left(\frac{\emptyset}{K_B T}\right)$$

Where T is the absolute temperature, $\emptyset$ is activation energy, K_B is Boltzmann constant and ρ_0 is resistivity at absolute temperature. After some calculations, we get the values of ρ_0 and $\emptyset$ which are (15.242 Ωm and 0.004 eV) and (19435.370 Ωm and 0.012eV) for PLZT50 and PLZT100 samples respectively. The reported activation energy for PLZT are 0.210, 0.124 and 0.136 eV for the x values of 0, 0.05 and 0.10 respectively (Prabhu et al 2013). Our calculated data are listed in the table 3, which indicates that increases of La^{+3} content increases the activation energy and resistivity which confirms the PLZT samples are relaxor type confirming the result obtained by XRD as well as dielectric data.

Table 3: Activation energy and resistivity for samples

S. No.	Sample	Ø (eV)	ρ_0(Ωm)
1	PLZT50	0.004	15.242
2	PLZT100	0.012	19435.370

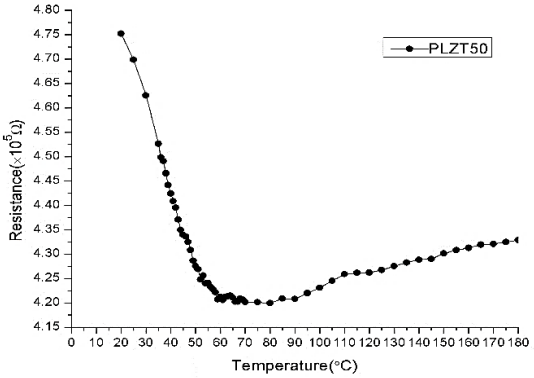

Figure 15: Variation of resistance with temperature for PLZT50 at frequency 100 KHz.

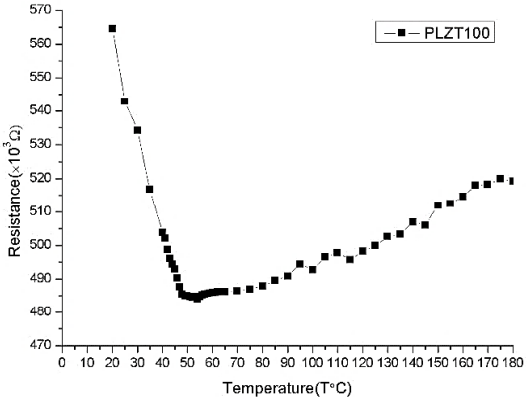

Figure 16: Variation of resistance with temperature for PLZT100 at frequency 100 KHz.

2. Cole-Cole Plot

The impedance provides thermally activated dielectric relaxation process in the materials and shows the reduction in bulk resistance with temperature. The opposite nature of variation of

$Z'$and Z'' i.e. static and dynamic with frequency and temperature reveals relaxor nature of materials. Figures (17 and 18) show the complex impedances spectrum (Z'vs Z'' called Nyquist or Cole-Cole Plot) of PLZT samples measured at temperature 155 °C as a function frequency (ranges from 100KHz to 1MHz).

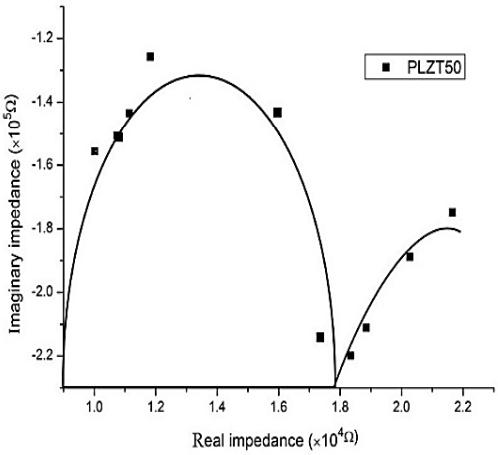

Figure 17: Cole-Cole plot between real and imaginary part of impedance for PLZT50 at temperature 155°C.

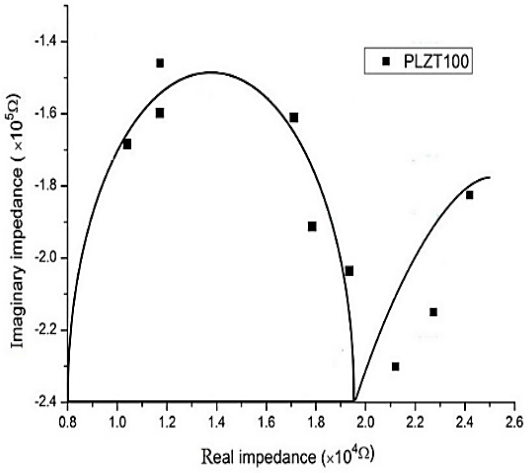

Figure 18: Cole-Cole plot between real and imaginary part of impedance for PLZT100 at temperature 155°C.

The impedance spectrum is characterized by appearance of semicircular arcs whose pattern of evolution changes with rise in temperature. This supports the increase in ac conductivity with temperature. In figure, the existence of double semi-circle is the indication of poly-dispersive type of the sample with double relaxation times in our samples, which are characteristics of ceramic relaxor (Jonscher et al 1983).

Conclusion

The electric properties of perovskite $Pb_{1-x}La_xZrTiO_3$ (x = 0, 0.5) ceramic prepared by dry route method were reported. The prepared highly dense above 96% of theoretical density PLZT ceramics were identified by X-ray diffraction method as a single cubic phase material with a perovskite structure having phase for both samples. The dielectric measurement was carried out as a function of both temperature (range 20°C to 180 °C) and frequency (100 KHz to 4 MHz). The peak value of dielectric data at 100 KHz are found to be at temperature 77°C and 48°C for PLZT50 and PLZT100 respectively. The peak value of temperatures at heating and cooling mode are different, which gives the low thermal hysteresis of 2°C and 1°C for PLZT50 and PLZT100 respectively. The existence of weak thermal hysteresis indicates the ferroelectric transition may be second order type or relaxor. The real part of dielectric constant is more than that of imaginary part. In the frequency dependence measurements the dielectric data decreases up to frequency 900 KHz in PLZT100 and 1 MHz in PLZT50 and then it starts increasing due to anomalous dispersion effect in the samples. The Curie temperature obtained from Curie Weiss behavior for PLZT50 and PLZT100 are 77°C and 41°C respectively. The observed values of Curie constant for PLZT50 and PLZT100 are; 602.002 °C and 680.166°C. The value of slope i.e. γ is 1.645 and 1.598, this confirm that the phase transition in PLZT samples tending towards diffuse or relaxor type. The activation energy and resistivity calculated from the Arrhenius Plot for PLZT samples are (0.004 eV and 15.242 Ωm), and (0.012 eV and 19435.370 Ωm) respectively. The existence of double semi-circle in Cole-Cole plots is the indication of poly-dispersive type of the samples with double relaxation times, which are characteristics of ceramic relaxor samples.

Acknowledgements

I would like to acknowledge the GoldenGate International College, Kathmandu, for the financial support. I also thank to Institute of Engineering Pulchowk for providing the facility of HIOKI (3532-50) LCR HI-TESTER and NAST for providing XRD facility.

References

Ahmad S., Panda R. K. and Janas V. F. 2011, "Ferroelectric ceramics: Processing, Properties and Application". Rutgers University journal.

Chelkowski A. 1994, "Dielectric Physics", Elsevier scientific Publishing Company, Oxford.

Cross L. E. 1987, Ferroelectrics **76**, 241-267.

Dai X., DiGiovanni A. and Viehland D. 1992, J. Appl. Phys. **79**, 1021-1029

Felix Y. L., Hwan R. J., Christopher S. L. and Laurent P. 2013, Smart Materials and Structures. **22,** 16.

Haertling G. H. 1999, J. Am. Ceram. Soc. **82**, 797-818.

Isupov V. A. 1975, Solid State Commun**., 17,** 1331.

Jaffe B., Cook W. R. and Jaffe H. 1971, Piezoelectric Ceramics. Academic Press, New York.

Jonscher A. K. 1983, "Dielectric Relaxation in Solid", Chelsea Dielectric Press, London.

Keve E. T. 2011, Ferroelectrics **10**, 169-174.

Liu. S. T., Heaps J. D. and Tufte O. N. 1972, "Ferroelectrics" **3**, 281-285.

Perantie J. 2014, "Electrical-field-induced dielectric and caloric effects in relaxor ferroelectrics," University of Olulu.

Prabhu M. 2013, "Studies of pure and doped lead zirconate titanate ceramics and pulsed laser deposited lead zicronate titanate thin films" Ph.D. Phys. Thesis, B. S. Abdur Rahman University.

Priya S. 2007, Electroceram. **19**, 165.

Shvartsman V., Kleemann W., Dec J. and Lu S. G. 2006, Appl.Phys. 99, 124111.

Uchino K. and Nomura S. 1982, "Ferroelectric Lett." **44**, 56.

Xu. Y. 1991, "Ferroelectric material and their Applications" North Holland, Elsevier science publication, Amsterdarm.

Yasuda N., Ohwa H. and Asano S. 1996, Jpn. J. Appl. Phys 35, 5099.

Zhi Y., Ang C., Guo R. and Bhalla A. S. 2002, J. Appl. Phys. **92**, 265.

Zhigang Z. and Gang Z. 1990, "Ferroelectrics" **81**, 43-54.